Two-Dimensional Transferred Nuclear Overhauser Effect Spectroscopy Study of the Conformation of MgATP Bound at the Active and Ancillary Sites of Rabbit Muscle Pyruvate Kinase†

Gotam K. Jarori,‡ N. Murali, and B. D. Nageswara Rao*

Department of Physics, Indiana University–Purdue University at Indianapolis (IUPUI), 402 North Blackford Street, Indianapolis, Indiana 46202-3273

Received February 9, 1994; Revised Manuscript Received April 11, 1994®

ABSTRACT: Pyruvate kinase binds one adenosine 5′-triphosphate (ATP) molecule at its active site and another at an ancillary site on each subunit. In order to determine the conformation of ATP bound at these sites, proton transferred two-dimensional nuclear Overhauser effect spectroscopy (TRNOESY) measurements were made at 500 MHz and 10 °C for several mixing times in the range 40–200 ms. The NOE values for the proton pair H1′–H2′ of ribose (which are 2.9 ± 0.2 Å apart, irrespective of nucleotide conformation) as a function of ligand concentration (1–10 mM ATP), with the ratio of ligand to enzyme being kept constant, indicate that at higher ligand concentrations adventitious binding of ATP at nonspecific site(s) makes a major contribution to the observed NOEs. When the ligand concentration is <2 mM, site-specific NOEs can be measured. Furthermore, addition of phosphoenolpyruvate (PEP) to the enzyme–MgATP sample results in competitive displacement of MgATP from the active site and reduces the observed NOE to that arising exclusively at the ancillary site, thus allowing the measurement of site-specific NOEs. The interproton distances determined from such site-specific NOE buildup curves were used as constraints in CHARMm to obtain the structure of MgATP. At the active site, MgATP has a glycosidic torsion χ = 44 ± 5° and the phase angle of pseudorotation for ribose P = 42.4°. At the ancillary site χ = 46 ± 5° and P = 127.6°. Thus the orientation of the adenine with respect to the sugar moiety is the same at both sites. However, the sugar pucker is quite different at the two sites; at the active site it is a ${}_4T^3$, whereas at the ancillary site it is a ${}_1T^2$. These results provide an explanation for the insensitivity of the TRNOE values for enzyme-bound MgATP to the addition of PEP in previous studies (Rosevear, P. R., Fox, T. L., & Mildvan, A. S. (1987) *Biochemistry 26*, 3487–3493; Landy, S. B., Ray, B. D., Plateau, P., Lipkowitz, K. B., & Nageswara Rao, B. D. (1992) *Eur. J. Biochem. 205*, 59–69). In both these studies the experiments were performed at high ligand concentrations, at which the observed NOEs are dominated by MgATP bound at weak nonspecific binding sites. Thus specific displacement of MgATP from the active site by the addition of PEP did not significantly alter the observed NOEs. By the same reasoning the NOE data in these studies could not provide correct conformational information. In the experiments presented here, the contribution from adventitious ligand binding at the nonspecific site(s) was circumvented by selecting appropriate ligand and protein concentrations. This experimental protocol has led to the determination of the site-specific conformations of MgATP at the active and ancillary sites on the enzyme.

Pyruvate kinase is one of the two enzymes that play the important role of manufacturing ATP[1] in anaerobic glycolysis. The enzyme has a molecular mass of 238 kDa, and it occurs as a tetramer of identical subunits. Among its special properties are that the enzyme requires for activation two divalent cations (Mg(II)) and one monovalent cation (K^+) per reaction complex, and that a second ancillary binding site exists for the nucleotide (ATP or ADP) in each subunit in addition to that at the active site (Mildvan & Cohn, 1966). The function of the ancillary site is not known. The reaction complexes of this enzyme have been subjected to extensive investigations for some time by a variety of techniques including NMR and ESR. Most of these studies (Sloan & Mildvan, 1976; Nageswara Rao et al., 1979; Lodato & Reed, 1987) were centered on the role of the divalent and monovalent cations, and on the nature of their binding especially in relation to the phosphate chains in the reaction complex. Recently two independent TRNOE studies of the conformation of enzyme-bound MgATP (Rosevear et al., 1987a; Landy et al., 1992) have been published.

Proton TRNOE (Balaram et al., 1972a,b; Clore & Gronenborn, 1982, 1983; Rosevear et al., 1981, 1983, 1987a,b; Landy et al., 1992) measurements were used by Rosevear et al. (1987a) to define the glycosidic orientation of the adenosine moiety in MgATP bound to pyruvate kinase. These authors attempted to differentiate MgATP bound at the active and the ancillary sites by making the measurements in the presence and absence of PEP on the basis that excess PEP displaces MgATP at the active site, while leaving that at the ancillary site undisturbed (Reynard et al., 1961). However, the NOE buildup curve for the proton pair H1′–H2′ (see Figure 1 for the numbering system used for the protons in MgATP), the internuclear distance for which is known to be unaffected by

† Work supported in part by grants from the National Institutes of Health (GM 43966) and IUPUI.

* Author to whom correspondence should be addressed.

‡ Present address: Biophysics group (SSP-NMR), Tata Institute of Fundamental Research, Homi Bhabha Road, Colaba, Bombay-400 005, India.

® Abstract published in *Advance ACS Abstracts,* May 15, 1994.

[1] Abbreviations: ATP, adenosine 5′-triphosphate; NOE, nuclear Overhauser effect; PEP, phosphoenolpyruvate; NMR, nuclear magnetic resonance; TRNOE, transferred NOE; TRNOESY, transferred two-dimensional nuclear Overhauser effect spectroscopy; tris-d11-Cl, tris(hydroxymethyl)aminomethane($-d_{11}$) with chloride as the counterion.

0006-2960/94/0433-6784$04.50/0

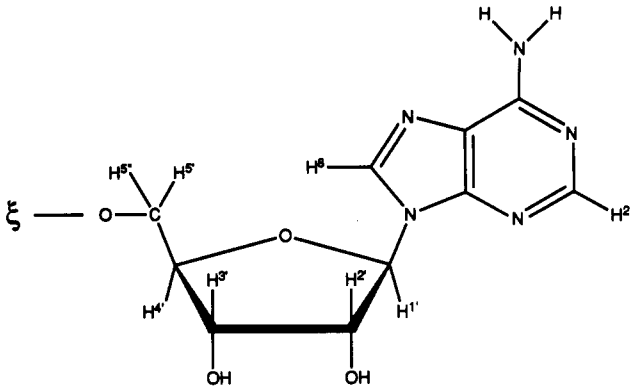

FIGURE 1: Adenosine moiety showing the numbering system used for the relevant protons.

variations in the sugar pucker and glycosidic rotation (Rosevear et al., 1983), showed no measurable change upon the addition of excess PEP to the sample (Figure 2c of Rosevear et al. (1987a)). Nevertheless, the results were analyzed in terms of a single conformation at the ancillary site and multiple conformations in fast exchange at the active site. Rosevear et al. (1987a) performed their TRNOE measurements in the 1D mode by monochromatic saturation of a desired resonance for a specified duration (τ_m), which was considered equivalent to a delay (or mixing time) by assuming instantaneous saturation. The results were analyzed on the basis of a two-spin approximation irrespective of the delay time.

Landy et al. (1992) investigated the conformation of MgATP bound to pyruvate kinase, as well as to the nucleotidyl transfer enzyme methionyl tRNA synthetase. The buildup of the TRNOE was measured once again in the 1D mode by employing a DANTE pulse for selective inversion (Morris & Freeman, 1978) of a chosen resonance followed by a delay time. These measurements also showed no measurable difference in the NOE upon the addition of excess PEP. The results were analyzed by the use of the complete relaxation matrix method applicable for the TRNOE experiments (Landy & Nageswara Rao, 1989). It was concluded that the experimental data is consistent with a single conformation for MgATP bound at all the sites with a glycosidic rotation angle of 39 ± 4° (Landy et al., 1992). This conformation also fit the TRNOE data for methionyl tRNA synthetase. Aside from the variance in the conformations deduced by these two investigations by Rosevear et al. (1987a) and Landy et al. (1992), the insensitivity of the observed TRNOE to the presence of excess PEP remained a puzzle (considering the fact that the displacement of MgATP at the active site by PEP was generally accepted).

Recent TRNOE measurements made in our laboratory on MgATP and MgADP bound to rabbit muscle creatine kinase (Murali et al., 1993) have drawn attention to the fact that nonspecific binding of the ligand to the enzyme might make a dominant contribution to the observed TRNOE for experimental sample protocols conventionally employed hitherto in such measurements including those by Rosevear et al. (1987a) and Landy et al. (1992). This aspect has not been previously investigated in sufficient detail, although it is not altogether unrecognized. The effects of nonspecific binding were demonstrated by Murali et al. (1993) by showing that the fractional NOE observed for H1′–H2′ for a fixed ratio of nucleotide and enzyme concentrations adequate to saturate the active sites increased significantly at high ligand concentrations. Furthermore, with such high nucleotide concentrations TRNOESY patterns similar to those for the creatine kinase–MgATP complexes were also obtained with proteins such as γ-globulin and bovine serum albumin which do not possess specific nucleotide binding sites. For enzyme (site) concentrations of about 1 mM, adventitious binding becomes significant when nucleotide concentrations are in excess of 5–10 mM. Under these conditions the excess nucleotide concentrations are large compared to the typical nonspecific dissociation constants of a few millimoles/liter. Thus, in order to minimize the effects of nonspecific binding it is necessary to determine the ligand concentration dependence of the observed TRNOE (keeping the ligand:protein ratio constant in the saturating range). An appropriate sample protocol with ligand concentrations sufficiently low such that the observed TRNOE arises predominantly from the specific binding may then be chosen.

In view of the results obtained by Murali et al. (1993), and considering the fact that in both of the previous studies by Rosevear et al. (1987a) and Landy et al. (1992) the sample protocols used are likely to allow for significant nonspecific binding of the nucleotide to the enzyme, we have reinvestigated the conformation of MgATP bound to rabbit muscle pyruvate kinase by making proton TRNOESY measurements. A proper sample protocol was developed by measuring the dependence of the observed TRNOE on nucleotide concentration, as discussed above. Since such a sample protocol assures that the observed NOE arises almost exclusively from the specific nucleotide binding sites, the question of the displacement of MgATP bound at the active site by PEP could be incisively addressed by making the measurements with and without PEP. Such measurements allowed a separation of the TRNOE contributions from nucleotide bound at the active and the ancillary sites. The results were then subjected to standard TRNOE analysis, followed by molecular mechanics calculations to determine the most acceptable conformations of MgATP at the two categories of sites.

EXPERIMENTAL PROCEDURES

Materials. ATP and PEP were obtained from Sigma Chemical Co. Rabbit muscle pyruvate kinase was from Boehringer Mannheim GMBH. Tris(hydroxymethyl)aminomethane-d_{11} and 99.99% D_2O were supplied by Research Organics Inc. All other chemicals used were of analytical reagent grade.

Preparation of Enzyme Sample. About 100 mg of the enzyme suspension was centrifuged, and the pellet was dissolved in 1 mL of 50 mM tris-d11 in 99.9% D_2O, and pH was adjusted to 8.0 by the addition of DCl. This solution was dialyzed against ten changes of the same buffer using a dialysis cell. After dialysis the enzyme was centrifuged, and the protein concentration was determined spectrophotometrically using $\epsilon_{280}^{mg/mL} = 0.54$ cm^{-1} and a molecular mass of 238 kDa. Pyruvate kinase is a tetramer with one catalytic site/subunit (Steinmetz & Deal, 1966). The enzyme concentrations reported here are in terms of subunits. The ATP concentration was measured using $\epsilon_{259}^{mM} = 15.4$ cm^{-1}. The pH values reported here correspond to the reading on a Beckman Altex Model 3500 digital pH meter and are not corrected for isotope effects.

NMR Measurements. ^{1}H NMR measurements at 500 MHz were made on a Varian Unity 500 NMR spectrometer. The solutions were in D_2O, and the sample temperature was maintained at 10 °C. NOESY time domain data were collected in the hypercomplex mode (States et al., 1982) with 256 t_1 increments and 2K t_2 points, with mixing times of 40, 60, 80, 120, 160, and 200 ms. Thirty-two scans were averaged

for each t_1 increment, and the zero-quantum interference was suppressed by random variation of the mixing time (up to 10% of its value) between different t_1 increments (Macura et al., 1981). A relaxation delay of 2 s was used in all the experiments. The carrier frequency was placed at the HDO resonance, which was suppressed by monochromatic irradiation using the decoupler channel during the relaxation delay, the t_1 period, and the mixing period. 2D Fourier transformations were performed with a Gaussian apodization on both dimensions and zero-filling to yield a 2K (F_1) × 4K (F_2) data set. The spectra were phased to the pure absorption mode. Fractional NOEs were determined by dividing the observed NOE volume by the diagonal peak volume of H1′ extrapolated to zero mixing time. In the experiments where measurements were made only for a single mixing time (80 ms), a control spectrum was recorded with zero mixing time. The diagonal volume of the H1′ resonance from such a control measurement was used to normalize the NOEs.

Theoretical Details. Data from a number of previous studies suggests that the lifetime of binary enzyme–nucleotide complexes is on the order of a millisecond (Jarori et al., 1985; Ray & Nageswara Rao, 1988; Ray et al., 1988; Jarori, et al., 1989). Similar estimates result on the basis of known dissociation constants (10^{-5}–10^{-4} M) and the assumption of diffusion controlled on rates of 10^8–10^9 M^{-1} s^{-1}. This lifetime is considerably shorter than proton relaxation times of 0.5–1.0 s in these complexes. The fast-exchange condition may, therefore, be assumed for TRNOE analysis. It has been shown that in the limit of fast exchange the characteristic equation for TRNOE is given by

$$\frac{d}{dt}\mathbf{m} = -\mathbf{R}\mathbf{m} \tag{1}$$

where $\mathbf{m}$ is a magnetization vector for all the spins and $\mathbf{R}$ is an average relaxation matrix given by

$$\mathbf{m} = \mathbf{m}^b + \mathbf{m}^f \tag{2}$$

$$\mathbf{R} = p_b\mathbf{W}^b + p_f\mathbf{W}^f \tag{3}$$

In eqs 2 and 3, $\mathbf{m}^b$ and $\mathbf{m}^f$ are n-component magnetization vectors, $\mathbf{W}^b$ and $\mathbf{W}^f$ are $n \times n$ relaxation matrices, and p_b and p_f are the population fractions for the bound and free ligand, respectively, each containing n spins (Landy & Nageswara Rao, 1989; Koning et al., 1990; Campbell & Sykes, 1991). The relaxation matrix elements of $\mathbf{W}^b$ and $\mathbf{W}^f$ are given by the standard expressions for the case of the dipolar interaction (Abragam, 1961; Noggle & Schirmer, 1971; Kalk & Berendson, 1976; Keepers & James, 1984; Landy & Nageswara Rao, 1989)

$$W_{ij} = W_{ji} = \frac{\gamma^4\hbar^2\tau_c}{10r_{ij}^6}\left[-1 + \frac{6}{1 + 4\omega^2\tau_c^2}\right] \tag{4}$$

and

$$W_{ii} = \frac{\gamma^4\hbar^2\tau_c}{10}\left[1 + \frac{3}{1 + \omega^2\tau_c^2} + \frac{6}{1 + 4\omega^2\tau_c^2}\right]\sum_{k\neq i} r_{ik}^{-6} \tag{5}$$

in which γ and ω are the gyromagnetic ratio and Larmor frequency of the protons, r_{ij} is the distance between spins i and j, and τ_c is the isotropic rotational correlation time. These parameters will correspond to the bound and free species depending on whether $\mathbf{W}^b$ or $\mathbf{W}^f$ is evaluated. The elements of $\mathbf{m}^b$ and $\mathbf{m}^f$ are given by analogous expressions, e.g.,

$$m_i^b = M_{zi}^b - M_{0i}^b \tag{6}$$

where M_{zi}^b is the instantaneous value of the z-component of the magnetization of spin i in the bound state and M_{0i}^b is its equilibrium value. Equations 4 and 5 assume that the spin system is in a single conformation characterized by the distances r_{ij} and is undergoing isotropic rotational diffusion characterized by τ_c. The intensity of the $i \leftarrow j$ cross peak in the two-dimensional TRNOESY experiment representing polarization transfer from j to i for a mixing time τ_m is given by

$$m_{i\leftarrow j}(\tau_m) = (e^{-\mathbf{R}\tau_m})_{ij}M_{0j} \tag{7}$$

$$= \left[\mathbf{1} - \mathbf{R}\tau_m + \frac{1}{2}\mathbf{R}^2\tau_m^2 - \frac{1}{6}\mathbf{R}^3\tau_m^3 + \ldots\right]_{ij}M_{0j} \tag{8}$$

Equation 8 shows that the buildup of the intensity of a cross peak given by $m_{i\leftarrow j}(\tau_m)$ vs τ_m in the TRNOESY spectrum is a polynomial in τ_m, and the initial slope of the buildup, which is just the linear term in eq 8, yields R_{ij}. If there are two binding sites (designated by (1) and (2)) for the ligand under fast-exchange conditions, R_{ij} is given by

$$R_{ij} = p_b(1)\,W_{ij}^b(1) + p_b(2)\,W_{ij}^b(2) + p_fW_{ij}^f \tag{9}$$

Since usually $(\omega\tau_c^b)^2 \gg 1$, $\tau_c^b \gg \tau_c^f$, and p_b/p_f is 0.1–0.25, the last term in eq 9 is negligible so that

$$R_{ij} \approx p_b(1)\,W_{ij}^b(1) + p_b(2)\,W_{ij}^b(2) \tag{10}$$

$$\approx R_{ij}^b(1) + R_{ij}^b(2) \tag{11}$$

TRNOE measurements under sample conditions in which both of the binding sites are occupied will yield R_{ij}. The distance information at the individual binding sites cannot be obtained unless it is possible to independently determine $R_{ij}^b(1)$ or $R_{ij}^b(2)$. In cases such as the ATP complexes of pyruvate kinase, if 1 and 2 represent the active and ancillary sites respectively, ATP at the active site may be displaced by adding a sufficient excess of PEP to the sample. TRNOE measurements on such a sample yield $R_{ij}^b(2)$. Thus by making the TRNOE measurements on ATP complexes of pyruvate kinase in the absence and presence of PEP, $R_{ij}^b(1)$ and $R_{ij}^b(2)$ may be evaluated and the interproton distances deduced for ATP bound at the active and ancillary sites.

It should be noted that eq 10 shows that the R_{ij}^b values at the two sites combine linearly to generate the effective relaxation matrix for the bound complex. However, the NOEs at the two sites are not additive except for short τ_m values for which eq 8 may be approximated to be linear in τ_m. The initial slopes of the buildup curves are, therefore, additive as indicated by eq 11. Values of R_{ij}^b at any particular site yield the ratios of interproton distances characteristic of that site through the relation

$$R_{ij}^b/R_{jk}^b = r_{jk}^6/r_{ij}^6 \tag{12}$$

Interproton Distance Constraints and Energy Minimization. For the determination of the ligand structure, the NOE-determined distances were used as constraints for energy minimization using the computer program CHARMm (Brooks et al., 1983) with the Powell minimization algorithm on a Silicon Graphics computer. The distance constraints were

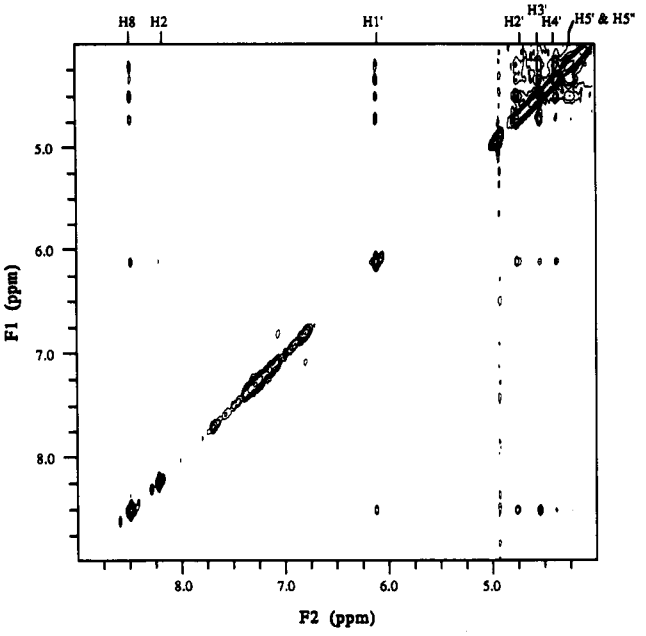

FIGURE 2: Proton TRNOESY spectrum (500 MHz) of pyruvate kinase–MgATP complex at 10 °C. The sample volume of 600 μL contained 0.199 mM enzyme sites, 1.05 mM ATP, 20 mM $MgCl_2$ in 50 mM tris-d11-Cl, pH 8.0 NMR parameters: 256 × $2t_1$ increments; 2K points during t_2; 32 transients for each t_1; mixing time, 160 ms; relaxation delay, 2 s. Two-dimensional Fourier transformation was performed along both dimensions with a Gaussian apodization and zero filling to obtain a 2K (F_1) × 4K (F_2) data set.

applied sequentially starting with the distances between H8 of the adenine ring and all of the ribose protons. In the second step, the distances between H1′ and all other sugar protons were added as constraints. In the final step, all of the 10–12 NOE determined distances were applied as constraints. A force constant F = 20 kcal mol^{-1} $Å^{-2}$ was used to obtain the initial structure that fit best with the experimental data. However, the energy of such an initial structure was significantly elevated. In order to refine the initial structure further, all the distance constraints were used again, but the force constant F was reduced to 10 kcal mol^{-1} $Å^{-2}$. This resulted in minor changes in the interproton distances, but the energy of the structure was lowered substantially.

RESULTS

Variation of TRNOE with Ligand Concentration. Role of Nonspecific Binding. A typical TRNOESY spectrum for a pyruvate kinase–MgATP sample is shown in Figure 2. The effect of ligand concentration on the observed intramolecular interproton NOEs was studied by recording such spectra at several different ligand concentrations with the enzyme to ligand ratio being kept constant. Initially a sample with 0.99 mM pyruvate kinase and a high ligand (MgATP) concentration of 10.08 mM was prepared. This sample was sequentially diluted with 50 mM tris-d11 buffer containing 20 mM $MgCl_2$ to obtainn different ligand concentrations with the ratio of ligand to enzyme concentration being kept constant. At each ligand concentration, TRNOESY spectra were recorded for mixing times of 80 and 0 ms (for normalization of NOEs). Figure 3 shows the change in percent NOE with increasing ligand concentration. The data are presented for NOE between H1′ and H2′ of ATP since the distance between these two protons (2.9 ± 0.2 Å) is independent of the nucleotide conformation (Levitt & Warshell, 1978; DeLeeuw et al., 1980; Rosevear et al., 1983). The fractional NOE is constant for ATP concentrations less than about 2 mM; however, at higher

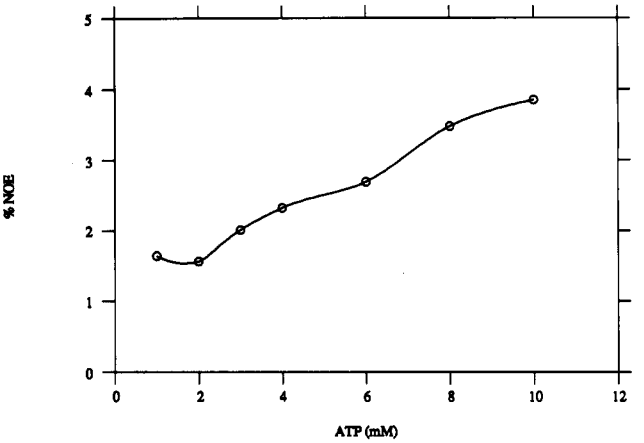

FIGURE 3: Dependence of percent NOE for the H1′–H2′ proton pair on ATP concentration in pyruvate kinase–MgATP complex. ATP concentration was varied from 1 to 10 mM, and the enzyme to ATP ratio was held constant at 1:10. The sample was in 50 mM tris-d11-Cl at pH 8.0, and measurements were made at 500 MHz and 10 °C with a mixing time of 80 ms. The NOEs were normalized by dividing the NOE peak volume with the diagonal peak volume of H1′ measured with zero mixing time.

concentrations it exhibits almost a linear increase. The smallest ATP concentration (1.0 mM) used here was large enough to saturate the active sites (0.1 mM) of pyruvate kinase in excess of 90% (K_d = 0.022 mM, Reed et al. (1970)). The large linear increase in NOE is clearly not due to the small increase of 10% in the saturation fraction at the active site. The dissociation constant for the ancillary site is not accurately known. However, it became clear from the measurements made in the presence of PEP (see below) that the ancillary sites are significantly populated at the lowest MgATP concentrations studied (~1 mM). Thus the nucleotide binding ancillary sites on the subunits are likely to be saturated for an MgATP concentration of about 2 mM. Since a linear increase of NOE is observed above this concentration, it must reflect a corresponding increase in the bound fraction of the ligand since the rotational correlation time and the H1′–H2′ distance remain constant. Such a linear increase in bound fraction of ligand with increasing ligand concentration is indicative of weak, nonspecific interactions of ATP with the enzyme. Thus the NOE measured at elevated concentrations will have contributions from binding at the specific as well as nonspecific binding sites. This observation is analogous to our recent TRNOESY studies on the Mg–nucleotide complexes of rabbit muscle creatine kinase (Murali et al., 1993).

NOE Buildup Curves for Structure Determination. For the determination of the bound ligand conformation at the active and ancillary MgATP sites, the experiments were performed at a ligand concentration of 1 mM and an enzyme subunit concentration of 0.195 mM. TRNOE measurements were made at several mixing times in the range 40–200 ms. Various intramolecular NOEs are clearly observable from the ligand. There were no observable off-diagonal NOE peaks between ATP and the enzyme protons (see Figure 2). In order to separate the NOEs arising from the active and ancillary binding sites of MgATP, the measurements were made in the absence and presence of PEP. Addition of a saturating amount of PEP resulted in the displacement of MgATP from the active site with a resultant decrease in the NOE. Since PEP also binds Mg(II), the divalent cation concentration was concomitantly increased so as to ensure that all the ATP was present as MgATP complex. The latter condition was ascertained by the coalescence of the H5′ and H5″ resonances. The buildup curves measured in the absence

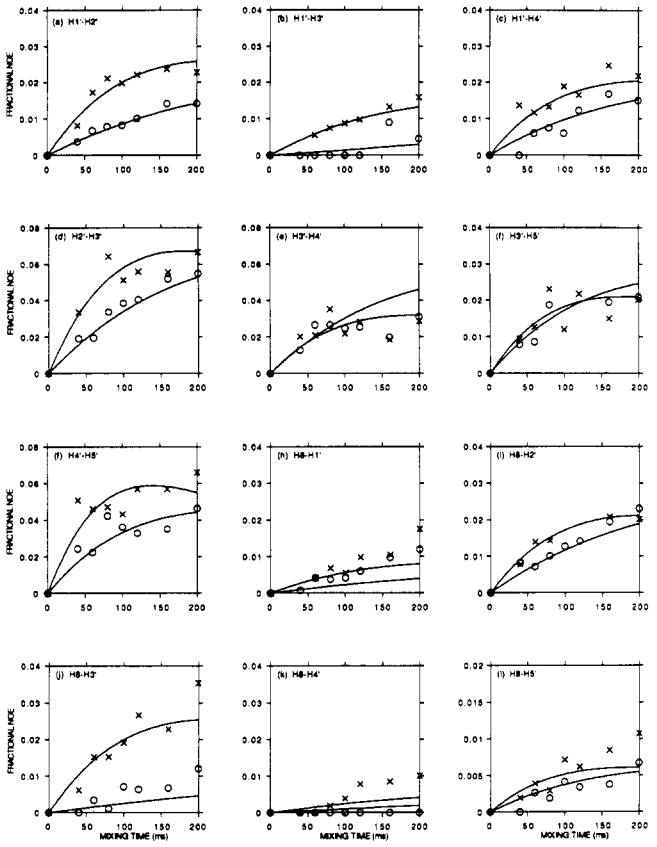

FIGURE 4: Fractional NOE buildup curves for pyruvate kinase–MgATP complexes. The sample contained 0.195 mM pyruvate kinase, 1.03 mM ATP, 39.2 mM $MgCl_2$, and 34.2 mM PEP in 50 mM tris-d11-Cl, pH 8.0. NOEs in the absence and presence of PEP are represented by × and ○, respectively. The solid curves represent theoretically simulated buildup curves based on the NOE matrix distances. External relaxation rates for H8, H2, H1′, H2′, H3′, H4′, H5′, and H5″ used in the fitting routine were 1.99, 1.23, 1.25, 2.11, 1.54, 2.0, 2.5, and 2.5 s^{-1}, respectively, at the active site, and for the ancillary site the external relaxation rates were 1.43, 1.23, 1.11, 1.43, 1.54, 2.0, 2.5, and 2.5 s^{-1}, respectively. The rotational correlation time used for the bound ligands was 11.5 ns.

and the presence of PEP are presented in Figure 4. In the absence of PEP the results represent the composite NOE arising from MgATP bound at both the active and ancillary sites, whereas those in the presence of PEP represent NOE arising exclusively from MgATP bound at the ancillary site. Although for most of the proton pairs a decrease in initial slope was observed upon the addition of PEP, there was no measurable change in NOE intensities between H3′ and H4′ (Figure 4e), indicating that there is no significant NOE between these two protons at the active site. On the other hand no NOEs were observed between H1′ and H3′ and between H8 and H4′ in the presence of PEP (Figures 4b,k), indicating that there is no significant NOE in these pairs at the ancillary site. The experimental data were fitted with a second-order polynomial to determine the initial slopes. As was shown by eq 10, the initial slope of the composite NOE curve is the sum of the initial slopes for the individual sites given by $R_{ij}^{b}(1)$ and $R_{ij}^{b}(2)$. The interproton distances were calculated from the initial slopes for both of the sites by using eq 12 and the reference distance of 2.9 Å between H1′ and H2′ (Rosevear et al., 1983). The R_{ij}^{b} values and distances derived in this manner are given in Table 1. The distances derived from these initial slopes were used as constraints to define the conformation of the nucleotide at the active site. For proton pairs that had no measurable NOE for mixing

Table 1: Initial Slopes for NOE Buildup in the Presence and Absence of PEP[a] and Interproton Distances in MgATP Bound at the Active and Ancillary Sites of Rabbit Muscle Pyruvate Kinase

	initial slope (s^{-1})			distances (Å)	
proton pair	no PEP	with PEP	active site	active	ancillary site
H1′–H2′	0.311	0.111	0.200	2.90	2.90
H1′–H3′	0.095	0.000	0.095	3.28	>4.5
H1′–H4′	0.227	0.126	0.101	3.25	2.84
H1′–H5′ and 5″	nd[b]	nd	nd	>4.00	>4.00
H2′–H3′	0.692	0.462	0.230	2.84	2.29
H2′–H4′	nd	nd	nd	>4.00	>4.00
H2′–H5′ and 5″	nd	nd	nd	>4.00	>4.00
H3′–H4′	0.429	0.392	0.037	3.84	2.35
H3′–H5′ and 5″	0.311	0.237	0.074	3.42	2.55
H4′–H5′ and 5″	0.694	0.453	0.241	2.81	2.29
H8–H1′	0.053	0.025	0.028	4.03	3.73
H8–H2′	0.272	0.141	0.311	3.11	2.79
H8–H3′	0.224	0.031	0.193	2.92	3.58
H8–H4′	0.021	0.000	0.021	4.24	>4.00
H8–H5′ and 5″	0.055	0.027	0.028	4.03	3.67

[a] The data are presented in Figure 4. [b] No detectable NOE. The distance between such proton pairs was set to be >4.00 Å.

times up to 120 ms, a nominal limiting value of 4.5 ± 0.5 Å was used for that interproton distance.

It may be noted from the initial slope data given in Table 1 that the values of R_{12}^{b} for the active site and ancillary site are given by 0.200 and 0.111 s^{-1}, respectively. From eqs 10 and 11 it is apparent that R_{ij}^{b} depends on three parameters: p_b, τ_c^b, and r_{ij}^b. The difference between the R_{12}^{b} values at the two sites may therefore arise due to a number of reasons such as the ancillary site being not as fully populated as the active site, or a slight difference within the experimental error of the r_{12} values (2.9 ± 0.2 Å) at the two sites, or some difference in the local mobility at the two sites leading to effective τ_c^b values that differ at the two sites, or a combination of all these factors. The data obtained in the present experiments cannot provide a discrimination between these factors. In the analysis, the r_{12} values at the two sites are nominally set equal to 2.9 Å, which leads to a ratio of 0.2:0.111 between the values of $p_b\tau_c^b$ at the active and ancillary sites. This does not affect the calculation of distances from the ratios of R_{ij}^{b} at individual sites. Values of R_{ij}^{b} at different sites are not used in the calculation. The distances given in Table 2 were used along with other parameters such as $p_b\tau_c^b$ in the complete relaxation matrix equation (eq 7) for TRNOE to compute the theoretical curves (solid lines) in Figure 4. In order to minimize the deviations between the experimental data and the computed values of NOEs for long mixing times (>120 ms), leakage terms have been added to the diagonal elements of the relaxation matrix (see caption of Figure 4). A single isotropic correlation time is used with the calculations of the relaxation matrix elements. Justification for such a description of the motion is available from ^{13}C line shape data of [2-^{13}C]ATP bound to several ATP-utilizing enzymes (Nageswara Rao & Ray, 1992).

Conformation of MgATP at the Active and Ancillary Sites. The interproton distances determined from initial NOE buildup rates (Table 1) were used as constraints in energy minimization calculations using the program CHARMm. A low-energy conformation consistent with the experimentally determined distances was chosen. Different interproton distances and various dihedral angles for the two structures are listed in Table 2. The interproton distances in the chosen energy-minimized structures deviated by no more than ±10% from the NOE-determined distances (see Table 2). The glycosidic torsion angle (χ) which defines the orientation of

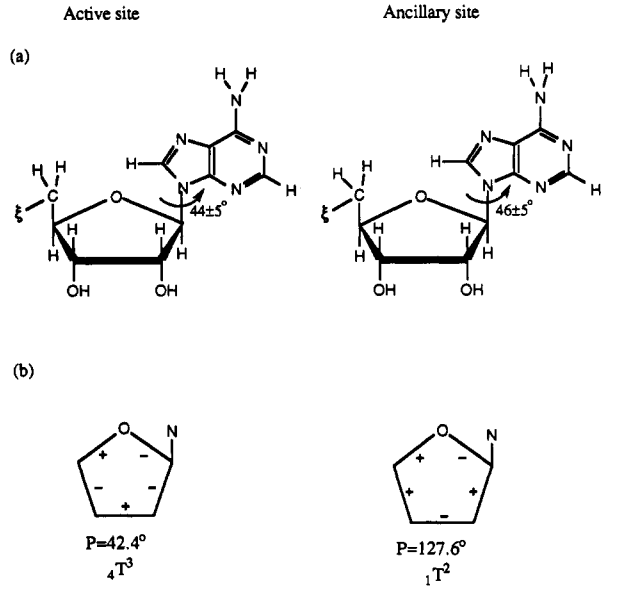

FIGURE 5: Schematic representation of the conformations of MgATP bound at the active and ancillary sites on pyruvate kinase. In part a the glycosidic torsion angle χ at both sites and in part b the sign of various torsion angles defining the sugar conformation and the phase angle of pseudorotation (P) are described.

adenine base with respect to ribose ring was found to be the same within experimental error at both sites (Figure 5a). However, the ribose conformation for MgATP bound at the two sites was quite different (Figure 5b); at the active site, it is characterized by a phase angle of pseudorotation P = 42.4° and amplitude of pucker τ = 28.4° corresponding to a $_4T^3$ pucker; at the ancillary site, P = 127.6° and τ = 22.1° corresponding to a $_1T^2$ pucker. These conformations fall within the preferred range of phase angles observed for β-purine glycosides (Altona & Sundaralingam, 1972).

DISCUSSION

An essential step in molecular structure determination by NOE measurements is to convert the observed NOE buildup curves into a set of interproton distances of the molecule. For intact systems this analysis of the NOESY data either by relaxation matrix or by initial slopes relies on the validity of two assumptions, viz., the existence of a single conformation for the molecule and the description of the molecular motion in terms of a single correlation time. For TRNOESY measurements there is an additional factor arising from the rate of exchange between the bound and free forms of the itinerant molecule (Clore & Gronenborn, 1982, 1983; Landy & Nageswara Rao, 1989; Ni, 1992; London et al., 1992; Lee & Krishna, 1992; Nirmala et al., 1992). If the exchange is fast, the data analysis is simplified (Landy & Nageswara Rao, 1989). For systems such as the nucleotide complexes of pyruvate kinase, the fast-exchange condition and the assumption of a single correlation time are reasonably valid (vide infra) so that the primary concern in accepting the TRNOE determined structure to be representative of the enzyme–substrate complex is the possibility that the NOE may be due to a superposition of the NOEs arising from multiple conformations in (fast) exchange. The multiplicity of conformations may arise, in general, from a conformational heterogeneity at a single binding site, or a conformational distinction between the substrate bound at different subunits or the presence of different classes of binding sites on each subunit such as the nucleotides at the active and ancillary sites of pyruvate kinase, or due to weak nonspecific binding of the nucleotide to the protein at sites other than the designated binding sites, or a superposition of all these features.

Table 2: Interproton Distances and Various Dihedral Angles for the Best-Fit Conformations of MgATP at the Active and Ancillary Sites of Pyruvate Kinase

	complete relaxation matrix		energy minimized	
proton pair	active site	ancillary site	active site	ancillary site
H1′–H2′	2.90	2.90	2.83	2.98
H1′–H3′	3.28	4.10	3.86	3.76
H1′–H4′	3.10	2.85	3.12	3.01
H1′–H5′	4.80	4.10	4.49	4.16
H1′–H5″	4.80	4.10	5.11	4.81
H2′–H3′	2.45	2.30	2.31	2.27
H2′–H4′	4.10	4.10	3.87	3.81
H2′–H5′	4.90	4.50	5.19	4.21
H2′–H5″	4.90	4.50	5.10	4.26
H3′–H4′	3.75	2.35	3.09	2.55
H3′–H5′	3.42	2.55	3.64	2.39
H3′–H5″	3.42	2.55	3.18	3.12
H4′–H5′	2.40	2.25	2.63	2.32
H4′–H5″	2.40	2.25	2.45	2.35
H8–H1′	3.65	3.65	3.88	3.77
H8–H2′	3.11	2.79	3.30	2.72
H8–H3′	2.75	3.60	2.70	3.62
H8–H4′	4.50	4.30	4.46	4.31
H8–H5′	3.85	3.30	3.84	3.27
H8–H5″	3.85	3.30	4.50	4.15

torsion angle[a]	active site (deg)	ancillary site (deg)
χ (O'_4–C'_1–N_9–C_8)	44	46
υ_0 (C'_4–O'_4–C'_1–C'_2)	−12	−21
υ_1 (O'_4–C'_1–C'_2–C'_3)	−6	21
υ_2 (C'_1–C'_2–C'_3–C'_4)	21	−13.5
υ_3 (C'_2–C'_3–C'_4–C'_5)	−28	1
υ_4 (C'_3–C'_4–C'_5–O'_4)	25	13
γ (O'_5–C'_5–C'_4–C'_3)	40	51
$P = \tan^{-1}\frac{(\upsilon_4 + \upsilon_1) - (\upsilon_3 + \upsilon_0)}{2\upsilon_2(\sin 36° + \sin 72°)}$	42.4	127.6 (−52.4)[b]

[a] For the definition of torsion angles and phase angle of pseudorotation (P), see Sanger (1984). The torsion angle χ (O'_4–C'_1–N_9–C_8) is 0° when the O'_4–C'_1 and N_9–C_8 bonds are eclipsed, and an anticlockwise rotation about the C'_1–N_9 bond is a positive angle rotation. [b] Since υ_2 is negative, 180° was added to the calculated value of P (see Altona and Sundaralingam (1972)).

In the present study the effects of weak, nonspecific binding were nearly eliminated by carefully optimizing the experimental conditions. It is assumed that the nucleotide binds with the same conformation at the active sites on all four subunits and binds likewise with a single conformation at the ancillary sites on these subunits. Thus we are reduced to two possibly distinct conformations: one for the active site and another for the ancillary site. The competition between PEP and ATP at the active site allows a separation of these two conformations by making measurements with and without PEP. As was explained in the introduction of this paper, previous attempts to effect such a separation by Rosevear et al. (1987a) and Landy et al. (1992) have resulted in no significant change in the observed NOE buildup curves for the H1′–H2′ proton pair. The two groups of authors have, however, interpreted the negative result differently. The results of the present work provide an explanation for the negative result in these two previous investigations. In both of these studies the experimental protocols used were such that there is appreciable weak, nonspecific binding of MgATP to the protein. The observed NOE in these experiments was thus dominated by the adventitious binding of MgATP and was, therefore, not significantly affected by the displacement of MgATP by PEP at the active site alone. On the other hand, in the present work the choice of the experimental

protocol limited the binding to the active and ancillary sites, and the displacement effect upon the addition of PEP can be clearly seen. These results illustrate the importance of a careful assessment of weak, nonspecific binding effects in TRNOE studies involving substrates such as the nucleotides, and the need for choosing experimental protocols that minimize the interference from such effects.

Since the strategy for minimizing adventitious binding effects is to work at sufficiently low nucleotide concentrations, the well-known advantage of using excess ligand concentrations to obtain high sensitivity in TRNOE measurements (Landy & Nageswara Rao, 1989; Campbell & Sykes, 1991) had to be sacrificed at least in part. However, the assured identity of binding site(s) is a compensating factor. In the analysis of the NOE data leading to the determination of the structures at the two sites (active and ancillary), polynomial fits leading to initial slopes had to be used. This was because the observed NOE is not a superposition of the NOEs at the individual sites in general. Such a superposition is only valid for very short mixing times, and only the initial slopes are linearly additive. The scatter in the data was a matter of concern. However, the acceptability of the initial slopes was checked by using all of the distances derived from the initial slopes in the complete relaxation matrix to trace the buildup of the experimental NOEs for all the proton pairs. Considering the limitation on the sensitivity imposed upon the experiment by the optimization of the sample protocol, and the complexity of the data analysis arising due to the two classes of binding sites, the general agreement between the buildup curves calculated by using the complete relaxation matrix and the experimental buildup curves is quite satisfactory.

The structures obtained for MgATP bound at the active and ancillary sites are quite similar in their glycosidic orientation. The major difference appeared in the sugar pucker defined by the angle P, which was 42.4° at the active site and 127.6° at the ancillary site. The glycosidic orientations (χ) obtained for the active and ancillary sites given by 44° and 46°, respectively, with an experimental error of ±5° are in good agreement with 51 ± 5° obtained for both MgADP and MgATP bound to creatine kinase (Murali et al., 1993). Rosevear et al. (1987a) proposed a C3′-endo ribose pucker with a high anti glycosidic torsional angle $\chi = 68 \pm 10°$ for MgATP bound at the ancillary site, and at the active site a superposition of three structures with (i) C3′ endo with χ = 30°, (ii) O1′ endo with $\chi = 55°$, and (iii) C2′ endo with χ = 217° were proposed. Landy et al. (1992) reported a C3′ endo with $\chi = 39 \pm 4°$ for MgATP at both sites for the same enzyme–nucleotide complex. Due to the high concentration sample protocol used, nonspecific binding effects contribute significantly in both of these earlier studies. The variance between these results and those reported here is not surprising. Although MgADP binds to pyruvate kinase at the same site as MgATP, it was not possible to study its structure in the enzyme complexes because the site-selective displacement of MgADP by PEP is not possible. The TRNOE data for MgADP will be a superposition of those from the two sites. If the data were to fit a certain structure, that structure would not represent MgADP bound at either the active or the ancillary site.

The correlation time obtained by analyzing the TRNOE data was about 11.5 ns, which is 10-fold smaller than that estimated from the Stokes–Einstein relation for a molecular mass of 238 kDa. This kind of discrepancy was observed in most TRNOE analyses (Rosevear et al., 1987a; Williams & Rosevear, 1991; Murali et al., 1993) and is generally ascribed to the loss of magnetization through pathways involving the protein protons (Nirmala et al., 1992; Murali et al., 1993). When ratios of initial slopes are used for evaluating the interproton distances, the correlation time drops out of the calculation. While this feature may provide some confidence in the data analysis, it is not obvious that the apparent reduction in NOE for every proton pair is scaled to nearly the same extent so that the ratios of initial slopes are virtually unaffected. In considering TRNOE-determined conformations it is useful to recognize the possible implications of this question.

ACKNOWLEDGMENT

The authors thank Dr. Bruce D. Ray, Operations Director, NMR Center, IUPUI, and Dr. Steven B. Landy for helpful discussions and Professor M. D. Kemple for a careful perusal of the manuscript. The use of computational facilities for molecular modeling at the Facility for Computational Molecular and Biomolecular Science, IUPUI, and helpful suggestions from Dr. Daniel H. Robertson are acknowledged.

REFERENCES

Abragam, A. (1961) *The Principles of Nuclear Magnetism*, Oxford University Press, London.

Altona, C., & Sundaralingam, M. (1972) *J. Am. Chem. Soc. 94*, 8205–8212.

Balaram, P., Bothner-By, A. A., & Dadok, J. (1972a) *J. Am. Chem. Soc. 94*, 4015–4017.

Balaram, P., Bothner-By, A. A., & Breslow, E. (1972b) *J. Am. Chem. Soc. 94*, 4017–4018.

Brooks, B. R., Bruccoleri, R. E., Olafson, B. D., States, D. J., Swaminathan, S. & Karplus, M. (1983) *J. Comput. Chem. 4*, 187–217.

Campbell, A. P., & Sykes, B. D. (1991) *J. Magn. Reson. 93*, 77–92.

Clore, G. M., & Gronenborn, A. M. (1982) *J. Magn. Reson. 48*, 402–417.

Clore, G. M., & Gronenborn, A. M. (1983) *J. Magn. Reson. 53*, 423–442.

DeLeeuw, H. P. M., Haasnoot, C. A. G., & Altona, C. (1980) *Isr. J. Chem. 20*, 108–126.

Jarori, G. K., Ray, B. D., & Nageswara Rao, B. D. (1985) *Biochemistry 24*, 3487–3494.

Jarori, G. K., Ray, B. D., & Nageswara Rao, B. D. (1989) *Biochemistry 28*, 9343–9350.

Kalk, A., & Berendson, H. J. C. (1976) *J. Magn. Reson. 24*, 343–366.

Keepers, J. W., & James, T. L. (1984) *J. Magn. Reson. 57*, 404–426.

Koning, T. M. G., Boelens, R., & Kaptein, R. (1990) *J. Magn. Reson. 90*, 111–123.

Landy, S. B., & Nageswara Rao, B. D. (1989) *J. Magn. Reson. 81*, 371–377.

Landy, S. B., Ray, B. D., Plateau, P., Lipkowitz, K. B., & Nageswara Rao, B. D. (1992) *Eur. J. Biochem. 205*, 59–69.

Lee, W., & Krishna, N. R. (1992) *J. Magn. Reson. 98*, 36–48.

Levitt, M., & Warshell, A. (1978) *J. Am. Chem. Soc. 100*, 2607–2613.

Lodato, D. T., & Reed, G. H. (1987) *Biochemistry 26*, 2243–2250.

London, R. E., Perlman, M. E., & Davis, D. G. (1992) *J. Magn. Reson. 97*, 79–98.

Macura, S., Huang, Y., Seuter, D., & Ernst, R. R. (1981) *J. Magn. Reson. 43*, 259–281.

Mildvan, A. S., & Cohn, M. (1966) *J. Biol. Chem. 241*, 1178–1193.

Morris, G. A., & Freeman, R. (1978) *J. Magn. Reson. 29*, 433–462.

Murali, N., Jarori, G. K., Landy, S. B., & Nageswara Rao, B. D. (1993) *Biochemistry 32*, 12941–12948.
Nageswara Rao, B. D., Kayne, F. J., & Cohn, M. (1979) *J. Biol. Chem. 254*, 2689–2696.
Nageswara Rao, B. D., & Ray, B. D. (1992) *J. Am. Chem. Soc. 114*, 1566–1573.
Ni, F. (1992) *J. Magn. Reson. 96*, 651–656.
Nirmala, N. R., Lippens, G. M., & Hallenga, K. (1992) *J. Magn. Reson. 100*, 25–42.
Noggle, J. H., & Schirmer, R. E. (1971) *The Nuclear Overhauser Effect*, Accademic Press, New York.
Ray, B. D., & Nageswara Rao, B. D. (1988) *Biochemistry 27*, 5579–5585.
Ray, B. D., Rosch, P., & Nageswara Rao, B. D. (1988) *Biochemistry 27*, 8669–8675.
Reed, G. H., Cohn, M., & O'Sullivan, W. J. (1970) *J. Biol. Chem. 245*, 6547–6552.
Reynard, A. M., Hass, L. F., Jacobsen, D. D., & Boyer, P. D. (1961) *J. Biol. Chem. 236*, 2277–2283.
Rosevear, P. R., Desmeules, P., Kenyon, G., & Mildvan, A. S. (1981) *Biochemistry 20*, 6155–6164.
Rosevear, P. R., Bramson, H. N., O'Brian, C., Kaiser, E. T., & Mildvan, A. S. (1983) *Biochemistry 22*, 3439–3447.
Rosevear, P. R., Fox, T. L., & Mildvan, A. S. (1987a) *Biochemistry 26*, 3487–3493.
Rosevear, P. R., Powers, V. M., Dowhan, D., Mildvan, A. S., & Kenyon, G. L. (1987b) *Biochemistry 26*, 5338–5344.
Sanger, W. (1984) *Principles of Nucleic Acid Structure* (Cantor, C. R., Ed.) pp 9–28, Springer-Verlag, New York.
Sloan, D. L., & Mildvan, A. S. (1976) *J. Biol. Chem. 251*, 2412–2420.
States, D. J., Haberkorn, R. A., & Ruben, D. J. (1982) *J. Magn. Reson. 48*, 286–292.
Steinmetz, M. A., & Deal, W. C. (1966) *Biochemistry 5*, 1399–1405.
Williams, J. S., & Rosevear, P. R. (1991) *J. Biol. Chem. 266*, 2089–2098.